nature medicine

Mutation of the COG complex subunit gene *COG7* causes a lethal congenital disorder

Xiaohua Wu[1,6], Richard A Steet[2,6], Ognian Bohorov[1], Jaap Bakker[3], John Newell[1,5], Monty Krieger[4], Leo Spaapen[3], Stuart Kornfeld[2] & Hudson H Freeze[1]

The congenital disorders of glycosylation (CDG) are characterized by defects in *N*-linked glycan biosynthesis that result from mutations in genes encoding proteins directly involved in the glycosylation pathway. Here we describe two siblings with a fatal form of CDG caused by a mutation in the gene encoding COG-7, a subunit of the conserved oligomeric Golgi (COG) complex. The mutation impairs integrity of the COG complex and alters Golgi trafficking, resulting in disruption of multiple glycosylation pathways. These cases represent a new type of CDG in which the molecular defect lies in a protein that affects the trafficking and function of the glycosylation machinery.

Protein glycosylation is ubiquitous and serves multiple functions[1]. The synthesis of *N*- and *O*-linked glycans requires numerous glycosyltransferases, glycosidases and nucleotide-sugar transporters localized in the endoplasmic reticulum and Golgi apparatus. The resident Golgi proteins are concentrated in specific cisternae of that organelle at a steady state, but they constitutively recycle through the endoplasmic reticulum[2]. The importance of proper glycosylation is illustrated by the autosomal recessive CDG. These multisystem diseases are caused by mutations in genes that encode proteins involved in the *N*-linked glycosylation pathway[3].

CDG are classified into two groups. Type I defects decrease the synthesis of the dolichol-linked $Glc_3Man_9GlcNAc_2$ precursor of *N*-linked glycosylation, which takes place in the cytosol and endoplasmic reticulum[3]. Type II defects impair subsequent trimming of the protein-bound oligosaccharide and addition of terminal sugars, which are carried out in the Golgi apparatus[3]. Because glycosylation occurs in all cells, it is not surprising that patients with CDG show multisystemic abnormalities. The most common clinical presentations shared by patients with CDG are mental retardation, seizures, hypotonia, liver malfunctions, coagulopathy and dysmorphia. Other less common symptoms include cerebellar hypoplasia, microcephaly and protein-losing enteropathy. Approximately 25% of CDG patients die from severe infections or multiple organ failure[4].

The isoelectric focusing (IEF) pattern of serum transferrin is abnormal in typical patients with CDG, providing a simple screening test for these disorders. Additional studies are required to define the precise defect. Here we present two siblings with a new form of CDG in which the defect is not in an enzyme or transporter directly involved in glycosylation, but rather in a protein that participates in the overall function of the Golgi apparatus.

RESULTS

Both patients had CDG-like clinical presentations

The male (P1) and female (P2) siblings were the fourth and sixth children of healthy consanguineous parents from the Mediterranean area. Their third child died shortly after birth with congenital defects similar to those of P1 and P2. Both had perinatal asphyxia and dysmorphia, including low-set, dysplastic ears, micrognathia, short neck and loose, wrinkled skin. Generalized hypotonia, hepatosplenomegaly and progressive jaundice developed shortly after birth. X-ray examination showed that P1 lacked humerus and tibia epiphysis, whereas P2 had short extremities. Computed tomography scan revealed that P1 had a large space at the cisterna cerebelli superior. P1 and P2 developed severe epilepsy and died at 5 and 10 weeks after birth, respectively, from recurrent infections and cardiac insufficiency.

Severe liver involvement suggested galactosemia and tyrosinemia, but these were excluded. Dysmorphic features might indicate a lysosomal storage disease. Multiple lysosomal enzymes were elevated in the circulation, but enzymatic assay excluded mucolipidosis II in P1. Coagulation factors were decreased in P2. Because patients with CDG share many clinical and biochemical features with these patients, we performed IEF analysis of their serum transferrin, which indicated abnormal glycosylation (**Fig. 1a**). A two- to fivefold reduction in total serum sialic acid in the patients further supported a generalized glycosylation defect, and a new type of CDG.

[1]The Burnham Institute, 10901 N. Torrey Pines Road, La Jolla, California 92037, USA. [2]Department of Internal Medicine, Washington University School of Medicine, 660 S. Euclid Ave., Saint Louis, Missouri 63110, USA. [3]Department of Clinical Genetics, Academic Hospital Maastricht, P. Debyelaan 25, 6229 HX Maastricht, The Netherlands. [4]Department of Biology, Massachusetts Institute of Technology, 77 Massachusetts Ave., Cambridge, Massachusetts 02139, USA. [5]Present address: Nestlé Research Center, Nestec Ltd., Vers–chez–les–Blanc, CH–1000 Lausanne 26, Switzerland. [6]These authors contributed equally to this work. Correspondence should be addressed to H.H.F. (hudson@burnham.org).

Published online 25 April 2004; doi:10.1038/nm1041

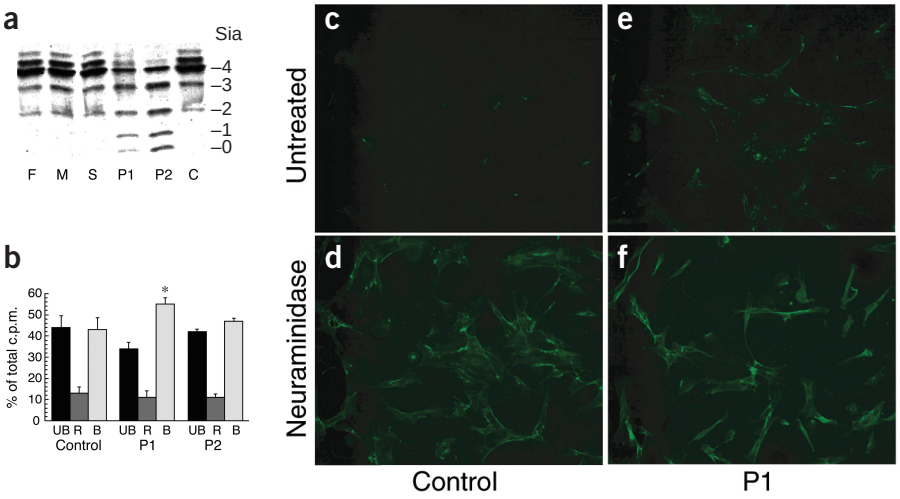

Figure 1 Alterations in protein glycosylation. (**a**) IEF of serum transferrin. F, father; M, mother; S, healthy sibling; P1 and P2, patients; C, control; Sia, number of sialic acids per molecule. (**b**) ConA pool I aliquots were subjected to RCA-1 agarose chromatography. Shown are fractions of total radioactivity with no RCA-1 affinity (UB, unbound), weak RCA-1 affinity (R, retained) and strong RCA-1 affinity (B, bound). c.p.m., counts per minute. Control, $n = 14$; P1, $n = 17$; P2, $n = 3$. *, $P < 0.001$. Error bars represent mean ± s.d. (**c**–**f**) PNA–Alexa Fluor 488 binding to control (**c**,**d**) and patient P1 (**e**,**f**) cells, before and after treatment with *V. cholera* neuraminidase. All images were obtained at ×100 magnification.

Alterations in patients' protein glycosylation

The abnormal transferrin IEF pattern showed an equal distribution of glycans with zero, one, two, three and four sialic acid residues as indicated (**Fig. 1a**), consistent with a type II CDG. The IEFs of the parents and healthy siblings were normal. To further determine whether *N*-linked oligosaccharide synthesis was abnormal in the patients' fibroblasts, we labeled them with [2-^{3}H]mannose and analyzed labeled glycopeptides on concanavalin A (conA)-Sepharose. Glycopeptides from patient and control cells fractionated identically, indicating that *N*-linked oligosaccharide branching was unaffected (data not shown). ConA-fractionated glycopeptides with highly branched sugar chains were then fractionated on a *Ricinus communis* agglutin-I (RCA-I) column (**Fig. 1b**). This lectin binds oligosaccharides with terminal galactose residues, but not those with galactose penultimate to terminal sialic acids. Glycopeptides from patient P1 showed a modest, significant ($P < 0.001$) increase in binding to RCA-I compared with normal samples, consistent with decreased sialylation, whereas those from patient P2 did not differ from controls. Digestion of all glycopeptides with an α2,3-specific neuraminidase increased lectin binding to >90%, indicating that nonbinding glycopeptides were modified with α2,3-linked sialic acid (data not shown). Thus, P1 fibroblasts had a partial defect in *N*-glycan sialylation.

Sialylation of cell surface *O*-linked glycans was also decreased in P1 fibroblasts (**Fig. 1c–f**). Normal fibroblasts showed negligible binding of fluorescent-tagged peanut lectin specific for terminal galactose residues on *O*-linked oligosaccharides (**Fig. 1c**). Neuraminidase treatment greatly increased staining, indicating that the lack of lectin binding resulted from the presence of sialylated *O*-linked glycans (**Fig. 1d**). Lectin staining of untreated P1 cells was readily detectable and increased after neuraminidase treatment, indicating a partial lack of sialylation of *O*-linked oligosaccharides (**Fig. 1e,f**). Because different sialyltransferases add sialic acid to *N*-linked and *O*-linked oligosaccharides[5], these findings suggested a general defect in sialic acid metabolism, such as synthesis, transport or use of cytidine monophosphate–sialic acid (CMP-Sia). To distinguish between these possibilities, we first assessed the level of CMP-Sia in normal and patient fibroblasts. P1 fibroblasts had a two- to threefold elevation of this nucleotide sugar, indicating the presence of sufficient cellular CMP-Sia (data not shown).

We next measured the transport of nucleotide sugars into the Golgi using streptolysin O–treated cells[6]. P1 fibroblasts transported [^{3}H]CMP-Sia, CMP-[^{3}H]Sia and uridine diphosphate UDP-[^{3}H]galactose into the Golgi at 30% of the normal rate (**Fig. 2a–c**). The integrity of Golgi cisternae was essential for transport, as coincubation with Triton X-100, which disrupts the Golgi membrane, completely prevented accumulation of label.

In addition, *in vitro* enzyme assays showed that P1 fibroblasts had reduced activity of two glycosyltransferases involved in the biosynthesis of *O*-linked oligosaccharides. The activities of Core1GalT and ST3Gal-I were 40% and 62% lower, respectively, than control

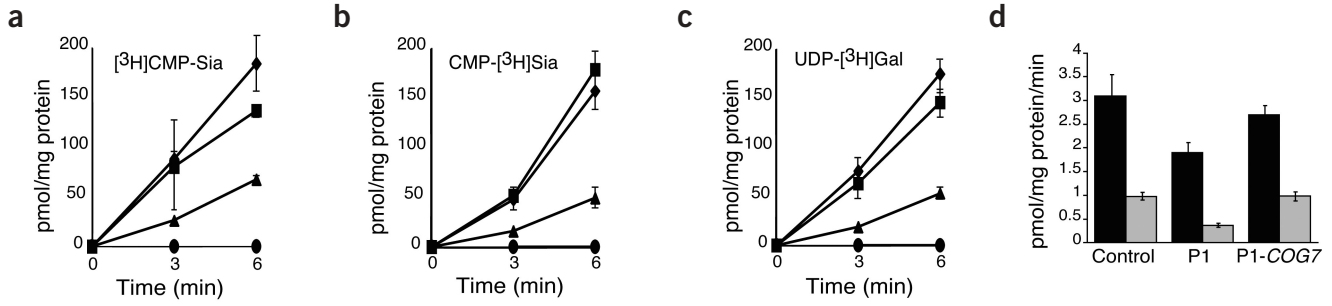

Figure 2 *COG7* mutation reduces activities of nucleotide-sugar transporters and glycosyltransferases. (**a–c**) Nucleotide-sugar transporters. Fibroblasts were permeabilized with streptolysin O and incubated with the indicated labeled sugar nucleotide. Results indicate the cell-associated product. ◆, control; ▲, P1; ■, P1-COG7; ●, Triton X-100. (**d**) Enzymes were assayed in cell lysates by incorporation of [^{3}H]galactose (Core1GalT; ■) and [^{3}H]sialic acid (ST3Gal-I; □) into added acceptors ($n = 3$). Data are presented as mean ± s.d.

(**Fig. 2d**). Thus, impaired *N*- and *O*-linked oligosaccharide synthesis in P1 fibroblasts seems to result from decreased activity of both nucleotide-sugar transporters and glycosyltransferases. Fibroblasts from P2 showed normal activity in all of these assays.

Golgi trafficking was altered in both patients

One mechanism that would account for the multiple defects in glycosylation in P1 fibroblasts is altered trafficking of proteins between the endoplasmic reticulum and the Golgi, and within the Golgi. This would lead to their mislocalization, impaired function and, possibly, enhanced turnover. Because the activity of ST3Gal-I was significantly decreased in P1 fibroblasts, we analyzed ST3Gal-I localization and trafficking by expressing a chimeric ST3Gal-I containing a green fluorescent protein (GFP) tag at the C terminus (ST-GFP). At steady state, ST-GFP expressed in normal and patient fibroblasts mostly colocalized with the Golgi marker GM-130 (data not shown). To assess trafficking, we photobleached Golgi ST-GFP and followed recovery of the fluorescent signal in the presence of cycloheximide to inhibit new protein synthesis. The rate of recovery is thus a measure of the movement of preexisting ST-GFP into the Golgi[7]. In control fibroblasts, detectable recovery of ST-GFP fluorescent signal in the Golgi began by 10 min, with strong recovery by 30–60 min (**Fig. 3**). Recovery of the Golgi ST-GFP signal was much slower in both P1 and P2 fibroblasts, indicating that the trafficking of Golgi-localized ST-GFP was affected in both patients. In contrast to the slow transport of ST-GFP in P1 cells, trafficking of the soluble lysosomal enzyme cathepsin D from the endoplasmic reticulum through the Golgi to the lysosomes was not altered (data not shown). This indicates that the defect in ST-GFP transport is selective.

Integrity of the patients' COG complex was impaired

The disruption of multiple glycosylation pathways in patient P1 fibroblasts is similar to that in the Chinese hamster ovary cell (CHO) mutants ldlB and ldlC[8]. These cell lines have mutations in genes encoding two subunits (COG-1 and COG-2, respectively) of the eight-subunit COG complex that is involved in protein transport within the Golgi and between the endoplasmic reticulum and the Golgi[9,10]. Loss of COG-1 and COG-2 results in destabilization of the complex and a failure of the residual subunits to localize to the Golgi in CHO cells[9,11,12].

Based on these similarities, we examined the localization of several COG subunits by indirect immunofluorescence. In normal fibroblasts, COG subunits 1–3 and 5–8 colocalized with the Golgi marker GM-130 (**Fig. 4a**, **Supplementary Fig. 1** online and data not shown). Both patients showed normal localization of COG-1 (**Supplementary Fig. 1** online), COG-2 and COG-3 (data not shown), but they had an abnormal distribution of COG-5 (**Fig. 4b**), COG-6 (**Supplementary Fig. 1** online) and COG-8 (data not shown), with diffuse cytoplasmic staining and little or no Golgi localization. COG-7 was undetectable in the fibroblasts of both patients (**Fig. 4a**), suggesting that lack of this subunit may represent their primary defect.

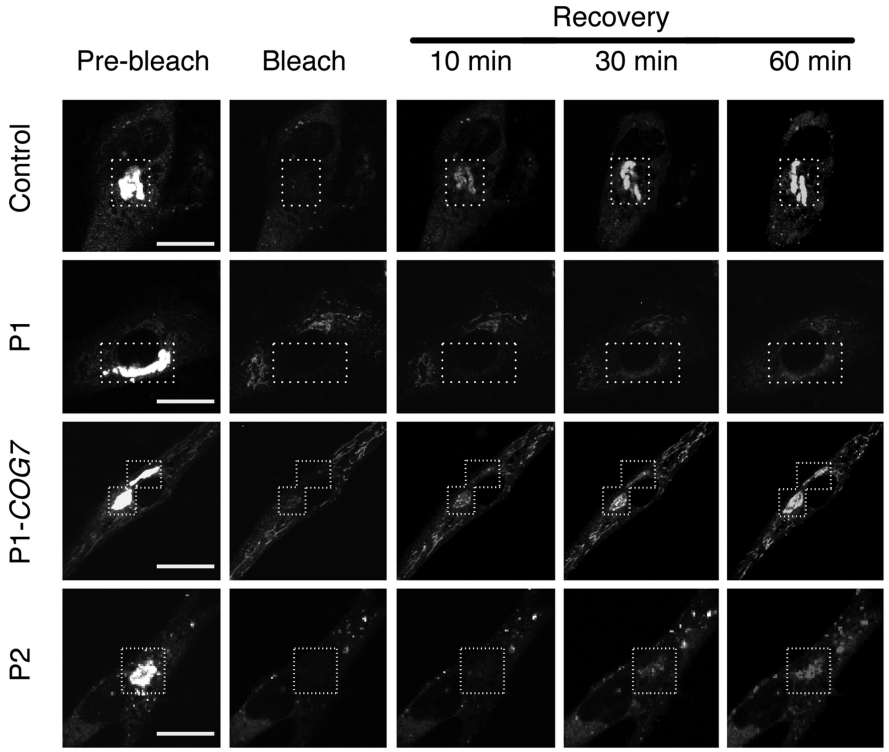

Figure 3 Trafficking of ST-GFP from endoplasmic reticulum to Golgi was impaired in patient fibroblasts. Fluorescence recovery after photobleaching experiments on normal fibroblast (Control), P1 fibroblast transfected with *COG7* cDNA (P1-*COG7*) and untreated P1 and P2 fibroblasts. Images are representative of three experiments with each cell type. Scale bars, 50 μm. Boxes indicate photobleached region.

A homozygous mutation in *COG7* alters its expression

To test this possibility, we sequenced *COG7* cDNA prepared from both patients' fibroblasts. The major species had a deletion of 19 bases corresponding to the last nucleotides of the first exon (**Fig. 5a**). Genomic DNA sequencing showed that both patients had a homozygous intronic mutation (IVS1+4 A→C; **Fig. 5b**) that was not found in 54 other unrelated individuals. This point mutation impairs splicing at the canonical site and allows the use of a cryptic, conserved alternative splicing site near the first exon/intron boundary (**Fig. 5c**), resulting in the 19-base deletion *CDG7* mRNA (**Fig. 5d**) and COG-7 protein (**Fig. 5e**) were reduced in both patients. The decreased *COG7* mRNA in the patients may result from reduced splicing efficiency, from production of a premature termination codon leading to mRNA degradation, or both. The patients' fibroblasts did contain a small amount of normal mRNA that was detected with primers that only amplify normal *COG7* mRNA (**Fig. 5f**). Western blots showed that the level of COG-7 was greatly reduced in the patients' cells relative to controls (by 95% in P1 and 85% in P2), whereas the content of GM-130 was the same in all cells (**Fig. 5e**). These values correlate with the levels of normal *COG7* mRNA in P1 and P2 cells (**Fig. 5d**,**f**).

Normal COG-7 rescues trafficking and glycosylation

To confirm that COG-7 deficiency was the primary defect, we introduced human wild-type *COG7* cDNA into the patients' fibroblasts using a retroviral expression system or a PHM6-HA-COG7 construct

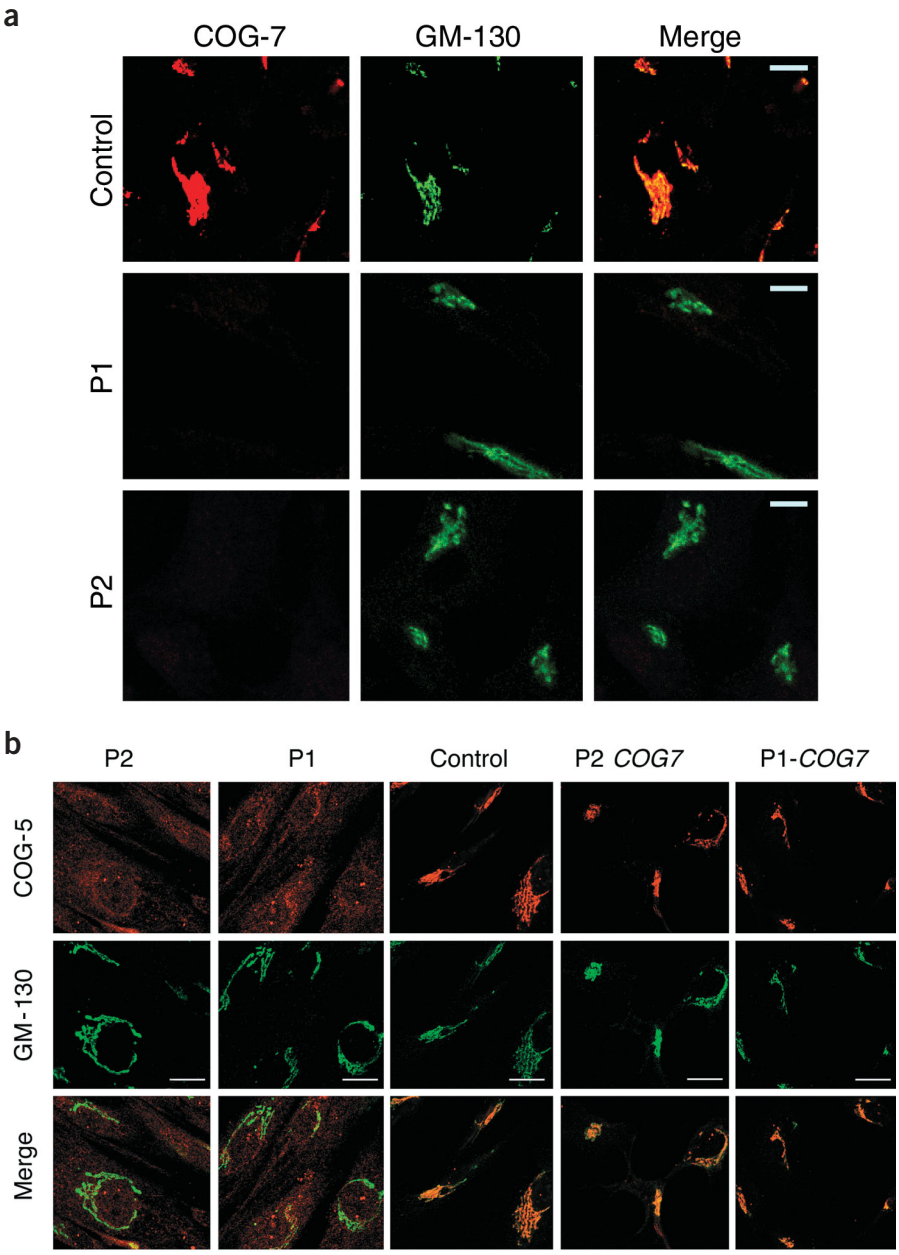

Figure 4 Integrity of patients' COG complex was impaired. (**a**,**b**) Immunofluorescence microscopy of control and patient fibroblasts (with or without transfection of PHM6-HA-COG7) was conducted using affinity-purified polyclonal antibody to COG-7 (**a**) or COG-5 (**b**) and a monoclonal antibody to Golgi marker GM-130. Scale bars, 50 μm.

(mammalian expression vector PHM6 containing hemagglutinin-tagged *CDG7*)[9]. *COG7* overexpression restored COG-5 Golgi localization (**Fig. 4b**) and corrected the glycosylation defects (**Fig. 5g,h** and **Supplementary Fig. 2** online). The activities of CoreIGalT and ST3Gal-I (**Fig. 2d**) and the CMP-Sia and UDP-Gal transporters (**Fig. 2a–c**) were also restored to control levels, and trafficking of the ST-GFP chimera was enhanced (**Fig. 3**). Transduction with the retroviral vector alone did not correct these abnormalities.

DISCUSSION

The COG complex is important in controlling Golgi-related membrane protein trafficking and localization in eukaryotes[8–17]. In yeast, deletion of *COG1*, *COG2*, *COG3* or *COG4* is lethal or greatly slows growth, whereas deletion of *COG5*, *COG6*, *COG7* or *COG8* permits growth but alters glycosylation and internal membrane organization[15]. *COG1* and *COG2* mutant CHO cells are viable, but exhibit defects in multiple Golgi glycosylation pathways[8,9], establishing a role for the COG complex in mammalian Golgi function. The siblings described here provide the first evidence that the COG complex mediates functions essential for survival in humans.

Despite having similar altered serum transferrin, glycosylation abnormalities and clinical courses, and identical mutations in *COG7*, only P1 showed altered glycosylation in fibroblasts. The most likely reason for this is that P2 fibroblasts made more normal *COG7* mRNA than P1 cells, increasing the amount of COG-7 protein and functional COG complex. As a result, P2 fibroblasts may have enough COG complex for normal glycosylation. Hepatocytes, which synthesize transferrin, and other organs presumably made insufficient COG-7 for adequate Golgi function, resulting in a severe multisystemic disease. The parental DNA was unavailable, but the results suggest that both were heterozygous for the same mutation, leading to an autosomal recessive disorder.

All known CDG cases so far have defects in genes encoding proteins directly involved in the synthesis of either glycoconjugates or sugar-donating molecules. The siblings described here define a new class of CDG in which the molecular defect lies in a protein that affects the trafficking of the glycosylation machinery. Because the COG abnormality probably affects many Golgi functions, some of the complications manifested by the siblings might have resulted from defects other than altered glycosylation. Many of their clinical symptoms, however, were similar to those seen in CDG patients.

Other patients will probably be identified with deficiencies in multiple glycosylation pathways. Some of these may result from mutations in *COG* or other genes that mediate intracellular trafficking and proper localization of the glycosylation machinery within the Golgi apparatus. Identifying these patients will first require analysis of serum transferrin[18] and apolipoprotein C–III[19] to confirm abnormal *N*- and *O*-linked glycosylation, respectively. Immunolocalization of COG, or possibly COG-sensitive, proteins[20] in patient fibroblasts may provide additional clues to the defects. Proper functioning of the glycosylation machinery may require a large number of proteins related to intracellular trafficking. Defects in many of them may also alter glycosylation.

COG deficiency may be considered a defect of either glycosylation or intracellular trafficking. The clinical presentations, biochemical features and diagnostic tools favor classification of the COG-7 defect as a glycosylation disorder. In contrast, no systematic nomenclature, common phenotype or diagnostic markers exist for intracellular trafficking

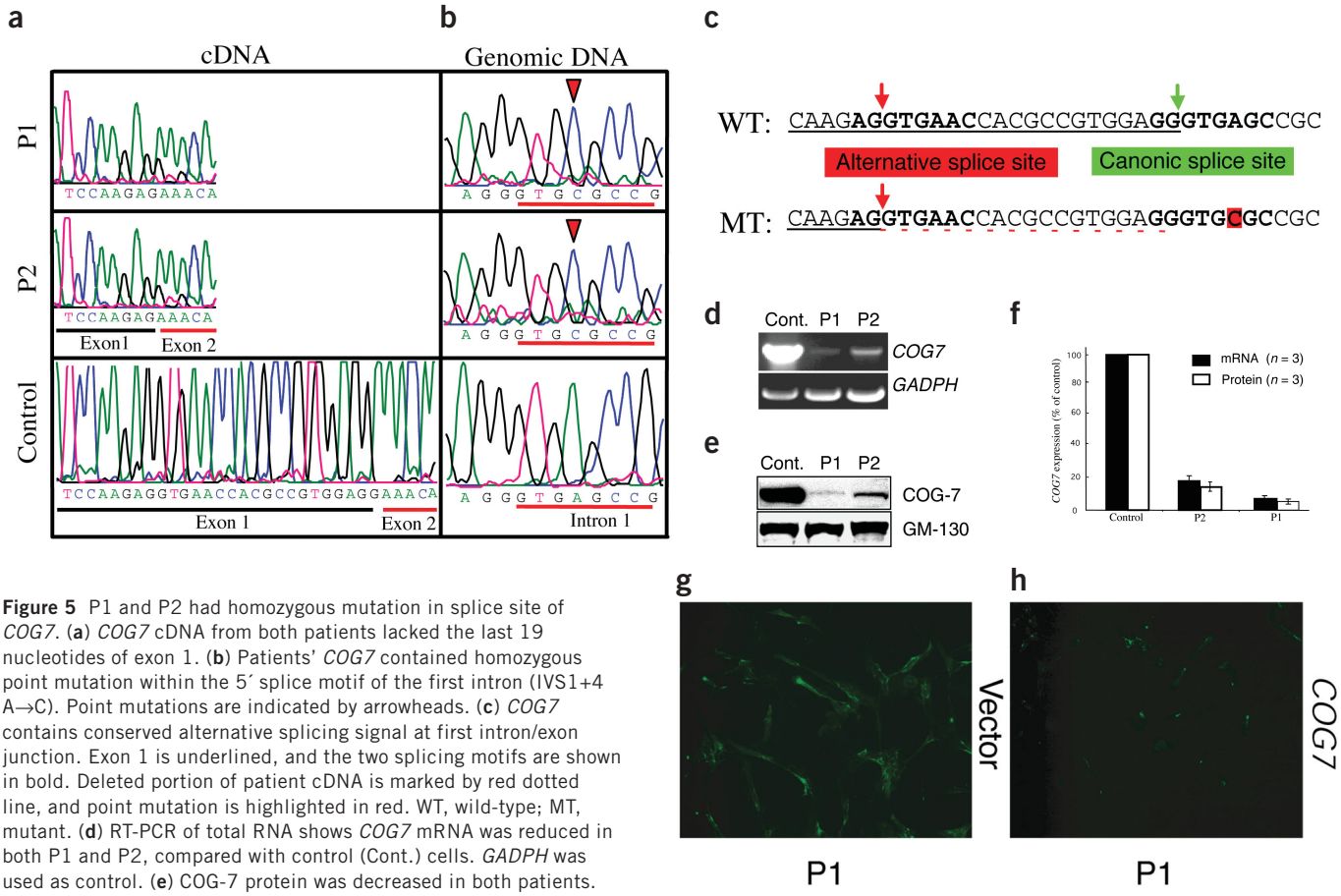

Figure 5 P1 and P2 had homozygous mutation in splice site of *COG7*. (**a**) *COG7* cDNA from both patients lacked the last 19 nucleotides of exon 1. (**b**) Patients' *COG7* contained homozygous point mutation within the 5′ splice motif of the first intron (IVS1+4 A→C). Point mutations are indicated by arrowheads. (**c**) *COG7* contains conserved alternative splicing signal at first intron/exon junction. Exon 1 is underlined, and the two splicing motifs are shown in bold. Deleted portion of patient cDNA is marked by red dotted line, and point mutation is highlighted in red. WT, wild-type; MT, mutant. (**d**) RT-PCR of total RNA shows *COG7* mRNA was reduced in both P1 and P2, compared with control (Cont.) cells. *GADPH* was used as control. (**e**) COG-7 protein was decreased in both patients. Western blots of COG-7 in P1, P2 and controls used 60 μg protein and Golgi marker (GM-130) as loading control. (**f**) Quantitative assay of *COG7* expression. Error bars represent mean ± s.d. (**g**,**h**) PNA-Alexa Fluor488 binding to P1 fibroblasts transduced with either vector (**g**) or wild-type *COG7* (**h**). Images were obtained ×100 magnification.

disorders[21–24]. We therefore propose that congenital defects that impair multiple glycosylation pathways resulting from disruption of Golgi trafficking should be classified as CDG. In keeping with current nomenclature, this disorder can be named CDG-IIe. We realize that this name is not optimal and may require revision as more glycosylation and trafficking disorders are discovered. Regardless of nomenclature, the most important issue is that the alteration of a patient's glycosylation status can reveal defects in intracellular protein trafficking.

METHODS

Materials. Reagents were obtained from Sigma, except conA-Sepharose (Amersham Biosciences), agarose-conjugated *Ricinus communis* lectin (Vector Laboratories) and Alexa Fluor 488–conjugated peanut lectin (Molecular Probes). Informed consent was obtained before skin biopsy for dermal fibroblasts, and experiments with patient materials followed guidelines of the Academic Hospital of Maastricht.

Radiolabels. [2-^{3}H]Mannose (24 Ci/mmol) was purchased from NEN. CMP-[^{3}H]Sia (33 Ci/mmol) and UDP-[^{3}H]Gal (30 Ci/mmol) were purchased from Perkin Elmer Life Sciences. [^{3}H]CMP-Sia (20.5 Ci/mmol) was synthesized from [^{3}H]CTP[25].

Antibodies. We used rabbit polyclonal antibodies to COG[9,11,13,20]. GM-130, a monoclonal antibody, was purchased from BD Transduction Laboratories.

Cell culture and transfections. Fibroblast growth has been described[6]. Transfection of 90% confluent cells with Lipofectamine 2000 (Invitrogen) and PHM6-HA-COG7 or pcDNA3 ST3Gal-I–GFP constructs was carried out according to the manufacturer's instructions.

Lectin analysis of *N*- and *O*-linked cell surface glycans. Lectin affinity analyses of glycopeptides have been described[26]. For *O*-linked glycans, cells were grown on polylysine-coated cover slips, treated with or without 50 mU *Vibrio cholera* neuraminidase for 1 h at 37 °C in culture medium, washed with PBS and fixed with 1% formaldehyde in PBS for 10 min at 23 °C. PBS-washed cover slips were incubated with 5 μg/ml PNA–Alexa 488 conjugate in 0.1% BSA/PBS (Molecular Probes) for 1 h at 23 °C, washed with PBS and visualized.

Determination of CMP-Sia acid levels. Intracellular levels of CMP-Sia and UDP–*N*-acetylglucosamine were determined by capillary electrophoresis. Fibroblasts were extracted with chloroform/methanol/water (1:2:0.8), incubated on ice for 10 min and centrifuged at 15,000 *g*. Chloroform/water (1:1) was added to the supernatants and centrifuged at 760 *g*. The upper (aqueous) layer was diluted to <5% methanol with water, lyophilized and redissolved in 250 μl water. Nucleotide sugars were analyzed using a P/ACE MDQ Glycoprotein System (Beckman-Coulter).

Mutation analysis. Total RNA and genomic DNA were purified using TRIzol reagent. RT-PCR used RNA as a template with Superscript One-Step RT-PCR System. RT-PCR primers (COG7-F01, 5′-AGTTACCCGTCCTGGCGTTT-3′; COG7-RO6, 5′-ATCTGTGCTGGTGAGTCGCGA-3′) were incubated at 50 °C for 40 min; 94 °C for 1 min; 40 cycles of 94 °C for 20 s, 55 °C for 20 s, 70 °C for 2 min; and 70 °C for 10 min. The RT-PCR products were either cloned into pCR2.1 vector or sequenced after separation on 1% agarose gels and purification with the Gel Extraction Kit. Three RNA prepa-

rations and independent RT-PCR reactions were carried out on the cDNA sequences. RT-PCR specific for wild-type *COG7* used primers COG7-WTF (5′-AAGAGGTGAACCACGCCGT-3′) and COG7-R02 (5′-GGCATCCGGT-CAATTTCAGT-3′). *GADPH* was used as control. PCR analysis of genomic DNA was done on P1, P2 and 54 unrelated individuals. The first exon/intron junction was amplified and sequenced in either direction with primers COG7-F02 (5′-ACTTCTCCAAGTTCCTGGCA-3′) and COG7-in-1 (5′-AGGGTATTTGCTGTCCATGC-3′).

Production of retrovirus. *COG7* cDNA was isolated from the cDNA library by RT-PCR with primer pairs 5′-CGGGATCCGGCAGTTCCGCCATG-GACTTCTCC-3′ and 5′-CGGAATTCCTTGGTGGTCCGGTGTGTGGTGG-3′. The 2.2-kb PCR product was subcloned into pCR2.1 vector (Invitrogen) and subcloned again into the ΔU3BstX retroviral vector. The ΔU3BstX vector was modified from ΔU3nlsLZ. Retrovirus was prepared by transient transfection of 293GPG packaging cells with the ΔU3COG7 construct, as described[27]. VSV-G-pseudotyped viral supernatants were collected from transfected packaging cells, and retroviral particles were concentrated by ultracentrifugation. *COG7* transgene expression in fibroblasts was controlled by multiplicity of infection.

Nucleotide-sugar transporter and glycosyltransferase assays. Streptolysin O–permeabilized cells were incubated with radiolabeled nucleotide sugars as described[6]. Reactions (100 μl) contained 0.1 μCi of CMP-[^{3}H]Sia, [^{3}H]CMP-Sia or UDP-[^{3}H]Gal. Cells were incubated for 0–6 min at 23 °C, diluted in 100 volumes of ice-cold PBS and centrifuged. Radioactivity in pellets was determined by $T = 0$ background subtraction. Core1GalT[28] and ST3Gal-I[29] assays have been described.

Determination of COG-7 levels. Fibroblasts (~95% confluence) were collected in PBS containing 1% Triton X-100 and protease inhibitors, and incubated on ice for 30 min. Protein (60 μg) was analyzed by SDS-PAGE on 4–20% gels and immunoblotted with antibodies to either COG-7 or GM-130. The blots were developed by ECL (Amersham Biosciences) and quantitated by densitometry.

Immunofluorescence microscopy. Cells were grown on eight-well Lab-Tek chamber slides for 12–24 h, washed with PBS, fixed in 3.8% paraformaldehyde in PBS for 10 min at 23 °C, and washed with PBS. The cells were permeabilized with 0.2% Triton X-100 in PBS for 10 min at 23 °C. For COG-5 staining, cells were treated with 6 M urea in PBS for 5 min, washed with PBS, blocked with 10% goat serum for 1 h and incubated for 1 h at 37 °C with primary antibody diluted in PBS with 5% goat serum. After PBS washes, FITC- or rhodamine-labeled secondary antibodies were diluted in 5% goat serum and incubated for 45 min at 37 °C. Slides were washed again with PBS and examined by laser-scanning confocal immunofluorescent microscopy (BioRad MRC-600).

Photobleaching recovery experiments. Fibroblasts were transiently transfected with ST3Gal-I–GFP construct and, 48 h after transfection, cycloheximide (10 μg/ml) was added to the medium 1 h before the imaging. Images were acquired with a 60× objective using an open pinhole diameter (10% transmittance) without saturation. Selective Golgi regions were bleached with high laser power (100% transmittance), and recovery was monitored at 5-min intervals.

Note: Supplementary information is available on the Nature Medicine website.

ACKNOWLEDGMENTS

We thank D. Ungar, T. Oka and V. Lupashin for purified COG antibodies; M. Ichikawa for technical support; B. Hayes and J. Kawakami for sugar nucleotide pool measurements; M. Fukuda for ST3Gal-I–GFP construct; D. Ory for assistance in preparing the retrovirus; and J. Sijstermans and S. van der Meer for clinical evaluation of the patients. This work was supported by grants RO1 DK55615 (H.H.F.), R37 CA08759 (S.K.), GM59115 (M.K.), U54 GM62116 and R24 GM61894, and by the March of Dimes Foundation (H.H.F.)

COMPETING INTERESTS STATEMENT

The authors declare that they have no competing financial interests.

Received 14 January; accepted 5 April 2004
Published online at http://www.nature.com/naturemedicine/

1. Varki, A. Biological roles of oligosaccharides: all of the theories are correct. *Glycobiology* **3**, 97–130 (1993).
2. Storrie, B. *et al.* Recycling of Golgi-resident glycosyltransferases through the ER reveals a novel pathway and provides an explanation for nocodazole-induced Golgi scattering. *J. Cell Biol.* **143**, 1505–1521 (1998).
3. Marquardt, T. & Denecke, J. Congenital disorders of glycosylation: review of their molecular bases, clinical presentations and specific therapies. *Eur. J. Pediatr.* **162**, 359–379 (2003).
4. Grunewald, S., Matthijs, G. & Jaeken, J. Congenital disorders of glycosylation: a review. *Pediatr. Res.* **52**, 618–624 (2002).
5. Schauer, R. Biosynthesis and function of *N*- and *O*-substituted sialic acids. *Glycobiology* **1**, 449–452 (1991).
6. Kim, S., Miura, Y., Etchison, J.R. & Freeze, H.H. Intact Golgi synthesize complex branched *O*-linked chains on glycoside primers: evidence for the functional continuity of seven glycosyltransferases and three sugar nucleotide transporters. *Glycoconj. J.* **18**, 623–633 (2001).
7. Lippincott-Schwartz, J., Roberts, T.H. & Hirschberg, K. Secretory protein trafficking and organelle dynamics in living cells. *Annu. Rev. Cell Dev. Biol.* **16**, 557–589 (2000).
8. Kingsley, D.M., Kozarsky, K.F., Segal, M. & Krieger, M. Three types of low density lipoprotein receptor-deficient mutant have pleiotropic defects in the synthesis of *N*-linked, *O*-linked, and lipid-linked carbohydrate chains. *J. Cell Biol.* **102**, 1576–1585 (1986).
9. Ungar, D. *et al.* Characterization of a mammalian Golgi-localized protein complex, COG, that is required for normal Golgi morphology and function. *J. Cell Biol.* **157**, 405–415 (2002).
10. Whyte, J.R.C. & Munro, S. Vesicle tethering complexes in membrane traffic. *J. Cell Sci.* **115**, 2627–2637 (2002).
11. Podos, S.D., Reddy, P., Ashkenas, J. & Krieger, M. LDLC encodes a Brefeldin-A sensitive, peripheral Golgi protein required for normal Golgi function. *J. Cell Biol.* **127**, 679–691 (1994).
12. Chatterton, J.E. *et al.* Expression cloning of LDLB, a gene essential for normal Golgi function and assembly of the ldlCp complex. *Proc. Natl. Acad. Sci. USA* **96**, 915–920 (1999).
13. Walter, D.M., Paul, K.S. & Waters, M.G. Purification and characterization of a novel 13 S hetero-oligomeric protein complex that stimulates *in vitro* Golgi transport. *J. Biol. Chem.* **273**, 29565–29576 (1998).
14. Loh, E. & Hong, W. Sec34 is implicated in traffic from the endoplasmic reticulum to the Golgi and exists in a complex with GTC–90 and ldlBp. *J. Biol. Chem.* **277**, 21955–21961 (2002).
15. Whyte, J.R. & Munro, S. The Sec34/35 Golgi transport complex is related to the exocyst, defining a family of complexes involved in multiple steps of membrane traffic. *Dev. Cell* **1**, 527–537 (2001).
16. Farkas, R.M. *et al.* The *Drosophila* COG5 homologue is required for cytokinesis, cell elongation, and assembly of specialized Golgi architecture during spermatogenesis. *Mol. Biol. Cell* **14**, 190–200 (2003).
17. Suvorova, E.S., Kurten, R.C. & Lupashin, V.V. Identification of a human orthologue of Sec34p as a component of the *cis*-Golgi vesicle tethering machinery. *J. Biol. Chem.* **276**, 22810–22818 (2001).
18. Freeze, H.H. Update and perspectives on congenital disorders of glycosylation. *Glycobiology* **11**, 129R–143R (2001).
19. Wopereis, S. *et al.* Apolipoprotein C–III isofocusing in the diagnosis of genetic defects in *O*-glycan biosynthesis. *Clin. Chem.* **49**, 1839–1845 (2003).
20. Oka, T., Ungar, D., Hughson, F.M. & Krieger, M. The COG and COPI complexes interact to control the abundance of GEARs, a subset of Golgi integral membrane proteins. *Mol. Biol. Cell* **15**, 2423–2435 (2004).
21. Olkkonen, V.M. & Ikonen, E. Genetic defects of intracellular-membrane transport. *N. Engl. J. Med.* **343**, 1095–1104 (2000).
22. Nichols, W.C. *et al.* Mutations in the ER-Golgi intermediate compartment protein ERGIC-53 cause combined deficiency of coagulation factors V and VIII. *Cell* **93**, 61–70 (1998).
23. Gedeon, A.K. *et al.* Identification of the gene (*SEDL*) causing X-linked spondyloepiphyseal dysplasia tarda. *Nat. Genet.* **22**, 400–404 (1999).
24. Zhang, B. *et al.* Bleeding due to disruption of a cargo-specific ER-to-Golgi transport complex. *Nat. Genet.* **34**, 220–225 (2003).
25. Blixt, O. *et al.* Efficient chemoenzymatic synthesis of *O*-linked sialyl oligosaccharides. *J. Am. Chem. Soc.* **124**, 5739–5746 (2002).
26. Steet, R.A., Melancon, P. & Kuchta, R.D. 3′-Azidothymidine potentially inhibits the biosynthesis of highly branched *N*-linked oligosaccharides and poly–*N*-acetyllactosamine chains in cells. *J. Biol. Chem.* **275**, 26812–26820 (2000).
27. Ory, D.S., Neugeboren, B.A. & Mulligan, R.C. A stable human-derived packaging cell line for production of high titer retrovirus/vesicular stomatitis virus G pseudotypes. *Proc. Natl. Acad. Sci. USA* **93**, 11400–11406 (1996).
28. Ju, T., Cummings, R.D. & Canfield, W.M. Purification, characterization, and subunit structure of rat Core1β1,3-galactosyltransferase. *J. Biol. Chem.* **277**, 169–177 (2002).
29. Gillespie, W., Kelm, S. & Paulson, J.C. Cloning and expression of the Galβ1,3GalNAc α2,3–sialyltransferase. *J. Biol. Chem.* **267**, 21004–21010 (1992).